Spectrum - The Journal of Operational Applications in Defense Areas

Journal homepage: https://spectrum.ita.br

Electronic Warfare and Remote Sensing: Analysis and Prediction of Military Target Signatures

Detection Capability of the X-47B UAV Aircraft Based on Static RCS Prediction

Newton A. S. Gomes[1] and Renan M. Richter[1]

[1]Aeronautics Institute of Technology - ITA, São José dos Campos/SP - Brazil

Article Info

Article History:

Received	15 May 2025
Revised	27 June 2025
Accepted	22 July 2025
Available online	23 September 2025

Keywords:

UAV
RCS
Radar Detection

E-mail adresses:

newtonsg@ita.br
richter@ita.br

Abstract

The doctrinal pillar "Combat Survival" is gaining increasing notoriety in the military environment. Recent conflicts, such as the Ukrainian War, as well as the clash between Azerbaijan and Armenia, indicate the increasing use of loitering munitions and UAVs (*Unmanned Aerial Vehicles*) as aerial attack platforms, reducing human contact on the front lines. This work performs the radar prediction of the X-47B UAV using electromagnetic simulations based on its static RCS (*Radar Cross Section*) in the VHF, L, S, C, and X frequency bands. A hypothetical radar evaluates the greatest detection ranges among the aforementioned bands. The results demonstrate that the VHF band obtained the greatest detection range, with a gain of 272.2% about the L band. Thus, the RCS analysis of an aerial platform with a delta-shaped flying wing geometry, such as the X-47B UAV, without electromagnetic absorbing materials, does not present stealth characteristics in the analyzed electromagnetic spectrum bands.

I. INTRODUCTION

The advent of unmanned aircraft has been revolutionary in the military, both in its conception and in its use [1]. In this context, UAVs have stood out in support and ground attack functions in conflict regions such as Afghanistan and, recently, in the war in Ukraine [2], [3]. However, the doctrine of the Air Forces of several countries lacks specific knowledge and information applied to control processes and, mainly, radar detection of these aerial structures at various electromagnetic frequencies [4].

Thus, this study proposes a methodology to evaluate the radar stealth level of the X-47B UAV combat aircraft. This function is performed based on the computational estimation of the RCS as a function of a set of engagement frequencies. Currently, due to the scarcity of information on the RCS of UAVs in the literature, especially those for military applications, this work aims to minimize this asymmetry in the technical-operational context of aerial combat.

The paper is divided as follows: Section II presents the theoretical basis, the RCS concept, and the radar equation. In addition, a brief history of the origin and development of the X-47B UAV will be presented. Section III discusses the modeling and simulation process of the X-47B UAV. Section IV presents the RCS of the X-47B as a function of frequencies and the prediction of the radar range. Finally, the conclusion of the work is presented.

II. THEORETICAL FOUNDATIONS

A. UAV X-47B

In the 1970s, a project to develop a UAV known as *Amber* was initiated at DARPA (*Defense Advanced Research Projects Agency*). This project gave rise to the MQ-1 *Predator* aircraft used by the US military, which began operations in 1995 [5].

In 1997, DARPA initiated the UCAV (*Uninhabited Combat Air Vehicle*) development program, in parallel with the USAF (*United States Air Force*), which sought to develop a multi-mission platform with a Suppression of Enemy Air Defenses (SEAD) capability. This effort resulted in the Boeing X-45A demonstrator, the first drone to autonomously launch an aerial weapons launcher [6].

In the 2000s, the USN (*United States Navy*) launched the UCAV-N (*Uninhabited Combat Air Vehicle - Naval*) program to develop a strike technology demonstrator capable of carrying a $1,814$ kg payload and ISR (*Intelligence, Surveillance, and Reconnaissance*) with an endurance of 12 flight hours and an operational radius of 650 NM, embarked on aircraft carriers. DARPA and the USN issued design contracts to Boeing and Northrop Grumman. Boeing responded with the platform designated X-46, based on the X-45 model, and Northrop Grumman introduced the X-47, Fig. 1 [6].

Northrop Grumman, using its resources, initially created a small proof-of-concept demonstrator called the X-47A *Pegasus*, which flew in 2003. Later, the X-47B was devel-

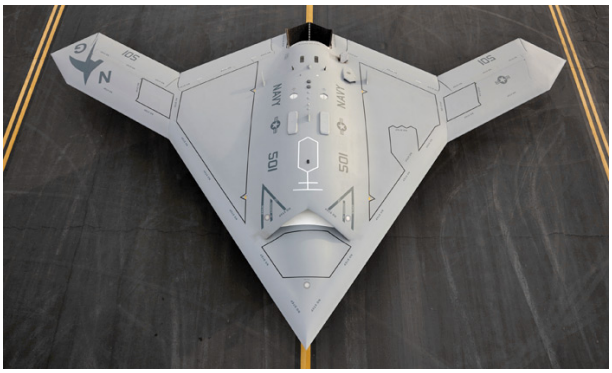

Fig. 1. X-47B UAV Aircraft [7].

oped from 2011 to 2015. The X-47B was the first UAV to take off and land from an aircraft carrier and to perform refueling in-flight autonomously. This aircraft achieved a balance between the aerodynamic capability for long-range flights and the structural strength, survivability, and low-speed flight stability, suitable for aircraft carrier operations, with radar stealth capability as one of the requirements [6].

B. Radar Equation and RCS

The concept of radar is associated with the propagation of electromagnetic waves, using Maxwell's equations [8]. A basic radar system consists of a transmitter, a receiver, and an antenna, emitting a set of pulsed microwave signals, where the electromagnetic energy transmitted by the antenna is defined by the *Poynting* vector $\vec{S}$ presented in (1) whose electromagnetic wave is composed of the electric field $\vec{E}$ and the magnetic field $\vec{H}$ [9].

$$\vec{S}(r,\theta,\phi) = \vec{E}(r,\theta,\phi) \times \vec{H}(r,\theta,\phi) \tag{1}$$

The *Poynting* vector corresponds to the directional density of the energy flux transferred per unit area, W/m^2, of an electromagnetic field in a given volume in space, at a specific frequency [10]. The operating principle of the radar corresponds to the detection of the energy flux scattered by the target, being detected by the radar receiver, which defines a maximum distance between this target and the radar by (2) [11].

$$R_{max} = \sqrt[4]{\frac{P_t G^2 \lambda^2 \sigma}{(4\pi)^3 k_B T_e B W F (SNR_o)_{min}}} \tag{2}$$

In this condition, the radar range is formatted for parameters inherent to the radar characteristics, such as the transmit power amplifier P_t, the antenna gain G, the emitted electromagnetic wavelength λ as a function of the operating frequency, the Boltzmann constant k_B, the system operating temperature T_e, the radar receiver bandwidth BW, the receiver noise figure F and the receiver signal-to-noise ratio SNR_o. The only independent variable of the radar system is the RCS σ of the target [9].

$$\sigma(\theta,\phi) = \lim_{r\to\infty} 4\pi r^2 \frac{\left|\vec{E}_s(r,\theta,\phi)\right|^2}{\left|\vec{E}_i(r,\theta,\phi)\right|^2} \tag{3}$$

As in (3), the RCS σ corresponds to the relationship between the electric field scattered by the target $\vec{E}_s$ and the electric field incident on the radar $\vec{E}_i$ as a function of the azimuthal ϕ and elevation θ angles. The RCS value in (3) is given in m^2, and the value in $dBsm$, defined by (4), is also used. RCS values, when below $1\,m^2$, are normally used in the unit of $dBsm$. This work uses the RCS values in $dBsm$ [9].

$$\sigma = 10 \cdot \log_{10}(\sigma\,[m^2])\ \ [dBsm] \tag{4}$$

III. MATERIALS AND METHODS

A. Modeling and Simulation of the X-47B UAV

The study of RCS of complex targets, such as a UAV, is carried out employing electromagnetic measurements in an anechoic chamber or by numerical computational methods using specific software for electromagnetic modeling and simulation [12].

The CAD (*Computer Aided Design*) was geometrically modeled by the software *FreeCAD* in the dimensions of 12.07 m in length, 19.0 m in wingspan, and 3.2 m in height [6], Fig. 2.

The software used in the study is FEKO® from ALTAIR, and the asymptotic RL-GO (*Ray Launching Geometrical Optics*) method is applied with discretizations (*mesh*) of $\lambda/10$ in CAD. All modeling and simulations were performed on an Intel Xeon E-2246 machine with 12 cores and 64 GB RAM.

(a)

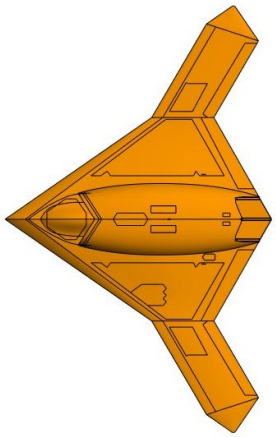

(b)

Fig. 2. (a) X-47B CAD side view. (b) X-47B top view.

The physical structure of the UAV is modeled with metallic conductive materials, known in the literature as PEC (*Perfect Electric Conductor*). In this material topology, the UAV is in the best-case configuration for detection, corresponding to the maximum reflection of electromagnetic

waves depending on the material used. This condition is essential to understanding the geometric effect of the aeronautical conformation as a function of the electromagnetic frequencies applied to its surface.

From the CAD imported into FEKO®, a *mesh* was applied to its PEC structure, obtaining a triangular mesh, Fig. 3, having a total of $42,108$ triangles with an average length of 0.10 m and a standard deviation of 0.06 m, whose maximum value was 0.23 m and a minimum value of 0.001 m.

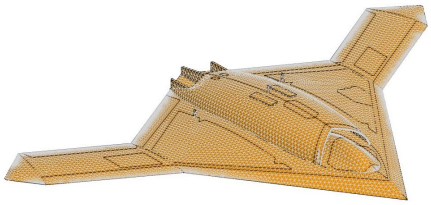

Fig. 3. Presentation of the *mesh* modeled in FEKO® for the X-47B UAV.

Evaluating the types of primary radars used worldwide for air defense and air traffic control used to detect aeronautical structures, the frequencies for electromagnetic simulations were defined, according to Table I.

Table I. Frequencies used in modeling and simulation processes.

Radar	Frequency [GHz]
VHF Band	0.18
L Band	1.32
S Band	2.80
C Band	5.30
X Band	10.0

Due to the type of mission for which the X-47B was designed, its radar threats are in land or naval areas. The monostatic radars allocated in these areas have a mechanical rotation around their axis or an electronic scanning; in this case, a *phased-array* radar [13].

In FEKO®, radar engagement modeling is performed using spherical coordinates, defining the azimuth angles ϕ and elevation angles θ, as shown in Fig. 4.

Radar engagement is performed with variations of θ and ϕ depending on the type of platform employed and the operational altitude of the UAV. In this work, the electric field vector $\vec{E}$ parallel to the XY plane of the UAV is used, Fig. 4, corresponding to a horizontal polarization of the HH type, which represents the emission of an electromagnetic wave in horizontal polarization and the detection of a scattered wave, originating from the target, in horizontal polarization.

IV. RESULTS AND DISCUSSION

A. *RCS of the X-47B UAV*

The radar stealth condition required to classify an aircraft or aerospace artifact is related to the numerical values of the RCS obtained as a function of the azimuth and elevation

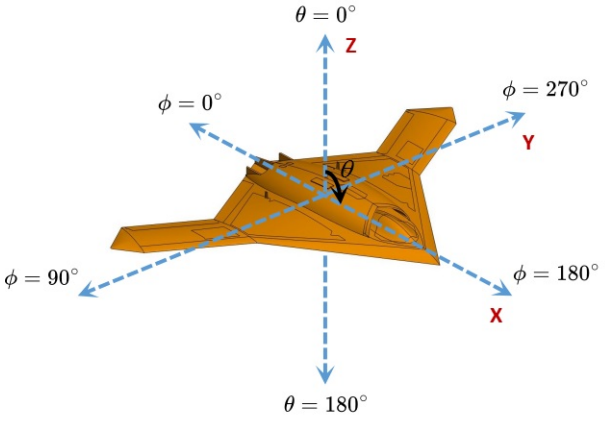

Fig. 4. Definition of azimuthal phi (ϕ) and elevation theta (θ) angles in the X-47B UAV model.

angles, as well as the engagement frequency. One classification used is LO (*Low Observability*) corresponding to an average RCS between -10 dBsm and -30 dBsm, and the VLO (*Very Low Observability*) condition corresponds to an average RCS with values below -30 dBsm [14].

Taking Fig. 4 as reference, the radar engagement is performed to evaluate the RCS of the X-47B in a radar beam at an angle of $\theta = 90°$ and a ϕ between $0°$ and $360°$. These results are presented in polar form, combining the VHF band with the other frequency bands in Fig. 5 (L band), Fig. 6 (S band), Fig. 7 (C band), and Fig. 8 (X band).

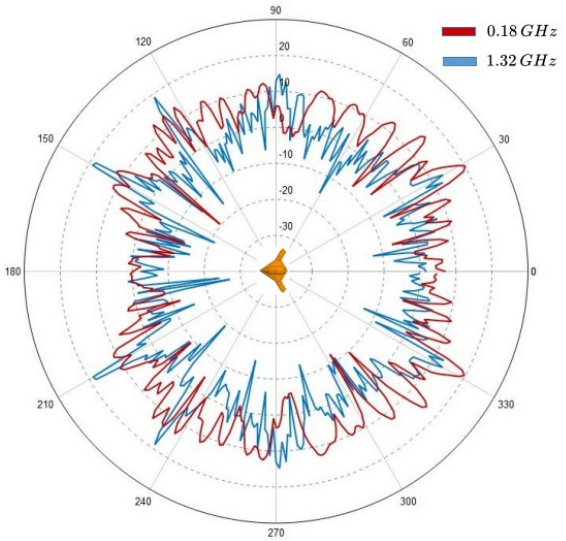

Fig. 5. RCS of the X-47B, in dBsm, at frequencies of 0.18 GHz and 1.32 GHz in polar form for $\theta = 90°$.

It is observed in Fig. 5, 6, 7 and 8 that the frequency of 0.18 GHz has a higher RCS than the other frequencies in several evaluated azimuths. At angles of $90°$ and $270°$ at the frequency of 0.18 GHz, the X-47B generates a reduced RCS in relation to the other frequencies used in the simulation.

To better understand the effect of RCS on the X-47B UAV, it is proposed to separate it into sectors, the radar engagement

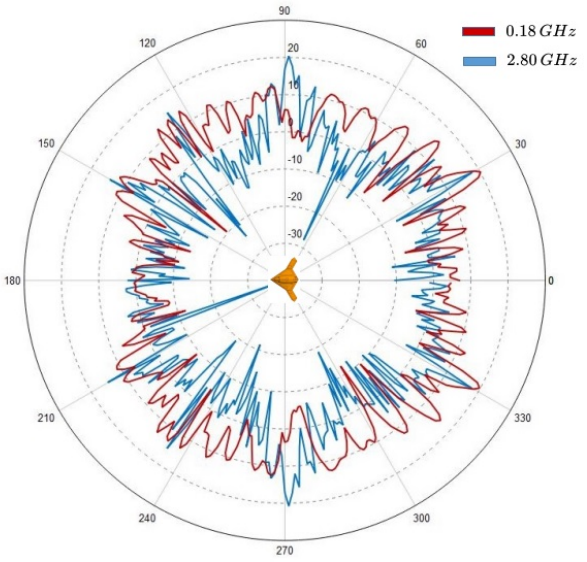

Fig. 6. RCS of the X-47B, in dBsm, at frequencies of 0.18 GHz and 2.80 GHz in polar form for $\theta = 90°$.

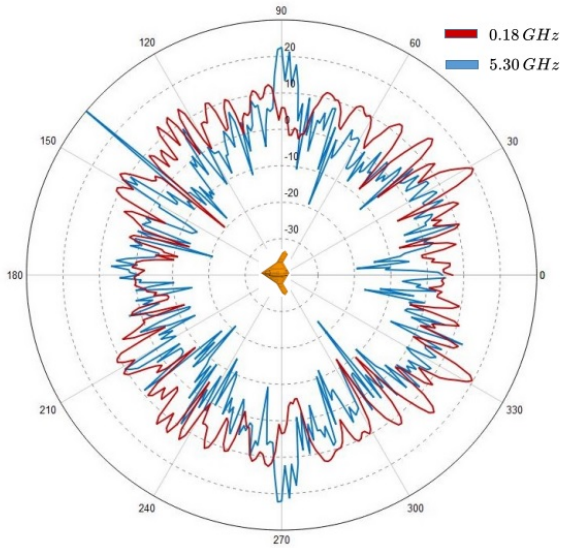

Fig. 7. RCS of the X-47B, in dBsm, at frequencies of 0.18 GHz and 5.30 GHz in polar form for $\theta = 90°$.

quadrants, as shown in Fig. 9.

The engagement quadrants are divided into four sectors, Fig. 9. Sector 1 has an azimuthal variation of $0° \leq \phi < 90°$, Sector 2 is $90° \leq \phi < 180°$, Sector 3 is $180° \leq \phi < 270°$ and Sector 4 is $270° \leq \phi < 360°$. From the definition of the engagement sectors, the mean values and standard deviation of the RCS are determined for each set of frequencies. These results are presented in Table II.

The RCS at frequencies of 1.32 GHz, 2.80 GHz, 5.30 GHz, and 10.0 GHz has a very similar average value for each sector evaluated. This condition implies that even when varying the emission frequencies, the RCS values obtained in the simulations are not very different in each engagement sector.

According to Table II, for the frequency of 0.18 GHz, the

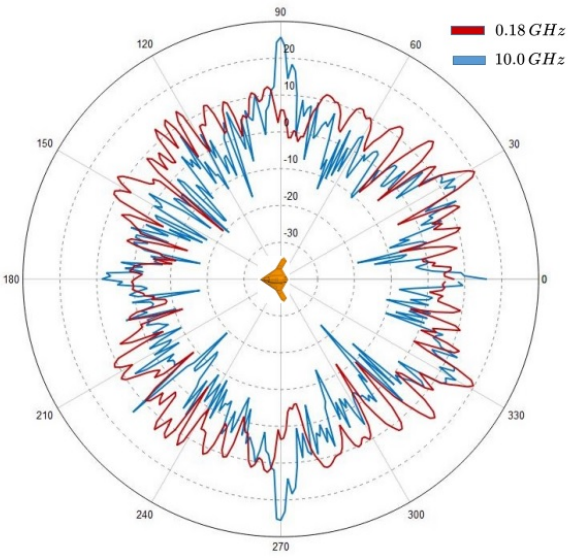

Fig. 8. RCS of the X-47B, in dBsm, at frequencies of 0.18 GHz and 10.0 GHz in polar form for $\theta = 90°$.

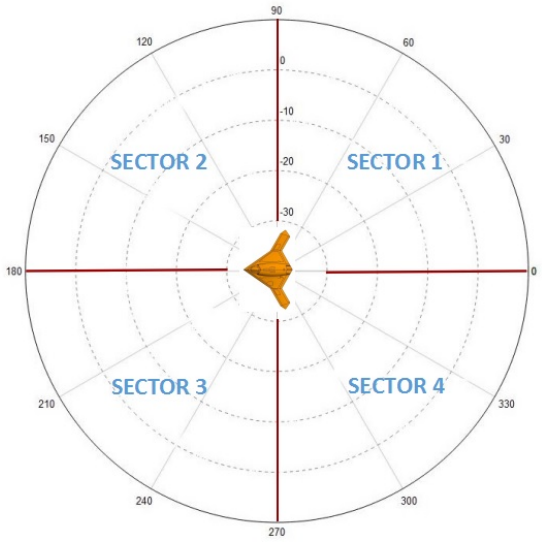

Fig. 9. Definition of radar engagement sectors for RCS analysis of the X-47B UAV.

Table II. Mean RCS values and standard deviation of the X-47B UAV as a function of engagement sectors.

Freq. [GHz]	Sector 1 [dBsm]	Sector 2 [dBsm]	Sector 3 [dBsm]	Sector 4 [dBsm]
0.18	6.82 ± 5.84	4.66 ± 6.47	4.65 ± 6.03	6.49 ± 6.28
1.32	1.29 ± 5.64	-1.07 ± 7.73	-1.18 ± 7.79	1.32 ± 5.93
2.80	1.43 ± 7.24	-2.94 ± 7.75	-2.28 ± 7.83	1.49 ± 7.00
5.30	0.72 ± 7.05	-1.19 ± 8.44	-2.16 ± 7.40	1.06 ± 7.55
10.0	1.94 ± 7.71	-2.12 ± 8.29	-1.32 ± 6.73	2.22 ± 8.20

RCS in the 4 evaluated sectors has values above the average RCS obtained at frequencies of 1.32 GHz, 2.80 GHz, 5.30 GHz, and 10.0 GHz.

It is important to note that these conditions are valid for an elevation angle of 90°, which corresponds to a low-altitude flight in relation to radar and the use of a metallic material in the construction of the X-47B.

The radar stealth criterion presented in this work is only achievable with the use of electromagnetic absorbing materials (RAM - *Radar Absorbing Materials*), incorporated into the aircraft structure, of the RAS (*Radar Absorbing Structure*) type [15]. In this case, for frequencies of 1.32 GHz, 2.80 GHz, 5.30 GHz, and 10.0 GHz, the material must attenuate at least, on average, 10 dB and for the frequency of 0.18 GHz, the attenuation value must be at least, on average, 20 dB.

Considering a hypothetical radar, keeping constant all variables attributed to the radar in the radar equation (2), at the frequencies evaluated in this work, the only variables are the wavelength λ and the RCS σ obtained from the electromagnetic simulations as a function of frequency. In (5), the value k corresponds to a constant of the hypothetical radar as a function of (2), with λ and σ being the variables used to estimate the probable maximum range R_{max}.

$$R_{max} = k \cdot \sqrt[4]{\lambda^2 \cdot \sigma} \tag{5}$$

By assigning a maximum range R_{max} for the frequency of 10 GHz in the value of 20 NM and applying (5) to the other frequencies, the values of R_{max} are estimated. The results of the maximum probable detection range as a function of the engagement frequencies are presented in Table III.

Table III. Probable range of X-47B engagement with a hypothetical radar.

Freq. [GHz]	0.18 [GHz]	1.32 [GHz]	2.80 [GHz]	5.30 [GHz]	10.0 [GHz]
R_{max}	210.6 NM	56.5 NM	37.6 NM	27.1 NM	20.0 NM

The results presented in Table III show that the L and S bands, used in air defenses, have a range gain to the C and X bands; however, the VHF band obtains a much higher range gain in relation to the L band, worth 272.7%.

V. CONCLUSION

This work presents a study of the RCS of the X-47B UAV in low-altitude flight conditions, in a stealth penetration profile in a multispectral radar environment, with frequencies in the VHF, L, S, C, and X bands.

Based on the engagements in the evaluated sectors, the RCS obtained as a function of the frequencies, angles θ and ϕ, and the X-47B UAV obtained high values in relation to the parameters that classify an aircraft as LO or VLO. In this case, under these modeling and simulation conditions, this aircraft cannot be considered stealthy to radar in the microwave range.

In order to meet radar stealth requirements, it is necessary to apply electromagnetic absorbing materials to its structure (RAS), prioritizing the greatest number of frequencies to be optimized in order to obtain a reduction in RCS of at least 10 dB.

The RCS prediction in the X-47B, at various engagement frequencies, shows high RCS values in the VHF band. This condition implies that radars in this band have a higher probability of detecting aircraft with stealth capabilities. When comparing the range obtained in the VHF band with the L band, the variation of RCS with an average value of 5 dB implies a variation in the detection range of 272.7%.

This work shows that the RCS analysis of an air platform with a geometry having a probable stealth capability, such as a delta-shaped flying wing, will not necessarily have effective radar stealth. It is desirable to carry out evaluations of the type presented in this work in order to obtain an initial predictability of this stealth capability and, if necessary, to point out the path for improvements in its aeronautical design.

VI. ACKNOWLEDGEMENTS

The authors thank the company ALTAIR for providing access to the FEKO® software throughout the electromagnetic modeling and simulation process.

REFERENCES

[1] W. W. Greenwood, J. P. Lynch, and D. Zekkos, "Applications of UAVs in Civil Infrastructure," *Journal of infrastructure systems*, vol. 25, no. 2, p. 04019002, 2019.

[2] R. Stojar, "The Drones and Issues Connected with Their Use in Contemporary Conflicts," in *International Conference Knowledge-Based Organization*, vol. 23, no. 1, 2017, pp. 305–310.

[3] M. Eslami, "Iran's Drone Supply to Russia and Changing Dynamics of the Ukraine War," *Journal for Peace and Nuclear Disarmament*, vol. 5, no. 2, pp. 507–518, 2022.

[4] A. G. Westra, "Radar Versus Stealth: Passive Radar and the Future of US Military Power," National Defense Univ Washington DC Inst For National Strategic Studies, Tech. Rep., 2009.

[5] DARPA, "UAV," Available at: https://www.darpa.mil/about-us/timeline/amber-predator-global-hawk-predator. Accessed on: October 18, 2024.

[6] J. Whittenbury, "Configuration Design Development of the Navy UCAS-D X-47B," in *AIAA Centennial of Naval Aviation Forum" 100 Years of Achievement and Progress"*, 2011, p. 7041.

[7] Lucas Karasinski, "Como seria a terceira guerra mundial na era high-tech," Available at: https://www.tecmundo.com.br/tecnologia-militar/22374-como-seria-a-terceira-guerra-mundial-na-era-high-tech.htm. Accessed on: May 28, 2024.

[8] D. J. Griffiths, *Eletrodinâmica*, 3rd ed. São Paulo: Pearson Addison Wesley, 2011.

[9] E. F. Knott, J. F. Schaeffer, and M. T. Tulley, *Radar Cross Section*. SciTech Publishing, 2004.

[10] C. Balanis, *Teoria de Antenas*. Rio de Janeiro: LTC, 2009, vol. 1.

[11] B. Mahafza, *Radar Signal Analisys and Processing using Matlab*, Alabama, 2009.

[12] M. Ezuma, C. K. Anjinappa, M. Funderburk, and I. Guvenc, "Radar Cross Section Based Statistical Recognition of UAVs at Microwave Frequencies," *arXiv preprint arXiv:2102.11954*, 2021.

[13] A. J. Fenn, D. H. Temme, W. P. Delaney, and W. E. Courtney, "The Development of Phased-array Radar Technology," *Lincoln Laboratory Journal*, vol. 12, no. 2, pp. 321–340, 2000.

[14] Air Power Australia, "A Preliminary Assessment of Specular Radar Cross Section Performance in the Chengdu J-20 Prototype," Available at: https://www.ausairpower.net/APA-2011-03.html#A.1. Accessed on: June 1, 2024.

[15] D. C. Silveira, N. A. S. Gomes, M. C. Rezende, and E. C. Botelho, "Microwave Absorbing Properties of Glass Fiber/Epoxy Resin Composites Tailored with Frequency Selective Surface based on Nonwoven of Carbon Fibers Metalized with Nickel," *Journal of Materials Science: Materials in Electronics*, vol. 31, pp. 13 095–13 103, 2020.